



Separation of postprandial lipoproteins: improved purification of chylomicrons using an ApoB100 immunoaffinity method

Grace Marie Jones,^{*} Russell Caccavello,[†] Sergiu P. Paliu,[†] Clive R. Pullinger,^{§,***} John P. Kane,^{§,††} Kathleen Mulligan,^{†,§§} Alejandro Gugliucci,^{1,2,†} and Jean-Marc Schwarz^{1,2,*,§§}

Departments of Basic Science* and Research,[†] College of Osteopathic Medicine, Touro University California, Vallejo, CA; Cardiovascular Research Institute[§] and Departments of Physiological Nursing^{**} and Biochemistry and Biophysics,^{††} University of California, San Francisco, San Francisco, CA; and Department of Medicine,^{§§} Division of Endocrinology, University of California, San Francisco, San Francisco, CA and Zuckerberg San Francisco General Hospital, San Francisco, CA

ORCID ID: 0000-0003-1106-0626 (G.M.J.)

Abstract Elevated levels of triglyceride-rich lipoproteins (TRLs), both fasting and postprandial, are associated with increased risk for atherosclerosis. However, guidelines for treatment are defined solely by fasting lipid levels, even though postprandial lipids may be more informative. In the postprandial state, circulating lipids consist of dietary fat transported from the intestine in chylomicrons (CMs; containing ApoB48) and fat transported from the liver in VLDL (containing ApoB100). Research into the roles of endogenous versus dietary fat has been hindered because of the difficulty in separating these particles by ultracentrifugation. CM fractions have considerable contamination from VLDL (purity, 10%). To separate CMs from VLDL, we produced polyclonal antibodies against ApoB100 and generated immunoaffinity columns. TRLs isolated by ultracentrifugation of plasma were applied to these columns, and highly purified CMs were collected (purity, 90–94%). Overall eight healthy unmedicated adult volunteers (BMI, 27.2 ± 1.4 kg/m²; fasting triacylglycerol, 102.6 ± 19.5 mg/dl) participated in a feeding study, which contained an oral stable-isotope tracer (^{1-¹³C acetate}). We then used this technique on plasma samples freshly collected during an 8 h human feeding study from a subset of four subjects. We analyzed fractionated lipoproteins by Western blot, isolated and derivatized triacylglycerols, and calculated fractional de novo lipogenesis. The results demonstrated effective separation of postprandial lipoproteins and substantially improved purity compared with ultracentrifugation protocols, using the immunoaffinity method. **■** This method can be used to better delineate the role of dietary sugar and fat on postprandial lipids in cardiovascular

risk and explore the potential role of CM remnants in atherosclerosis.—Jones, G. M., R. Caccavello, S. P. Paliu, C. R. Pullinger, J. P. Kane, K. Mulligan, A. Gugliucci, and J.-M. Schwarz. Separation of postprandial lipoproteins: improved purification of chylomicrons using an ApoB100 immunoaffinity method. *J. Lipid Res.* 2020. 61: 455–463.

Supplementary key words triacylglycerol • stable-isotope tracer • mass spectrometry • immunoaffinity • apolipoprotein B100 • chylomicrons

Elevated levels of fasting plasma triacylglycerol (TAG) have been recognized as a risk factor for coronary heart disease, which, in turn, increases the risk of myocardial infarction (1–3). In the 1970s, Zilversmit (4) postulated that processes that cause atherosclerosis might occur during the postprandial period and that dietary lipids transported by chylomicrons (CMs) were an important contributor to cardiovascular risks. While Parks et al. (5) were able to demonstrate that the flux of VLDL is greater during fasting versus the postprandial state, the role of CMs has yet to be elucidated. More recently, dietary sugars, specifically fructose, have been shown to increase TAG with supportive evidence that hepatic conversion of dietary sugars to

This work was supported by National Institutes of Health Grants HL113887, DK089216, and DK078153, as well as by Touro University California. C.R.P. and J.P.K. were supported by the Joseph Drown Foundation, the Campini Foundation, and by gifts from Peter Read, Harold Dittmer, Susan Boeing, and Donald Yellon. The content is solely the responsibility of the authors and does not necessarily represent the official views of the National Institutes of Health. The authors declare that they have no conflicts of interest with the contents of this article.

Manuscript received 8 May 2019 and in revised form 23 December 2019.

Published, JLR Papers in Press, December 30, 2019

DOI <https://doi.org/10.1194/jlr.D119000121>

Copyright © 2020 Jones et al. Published under exclusive license by The American Society for Biochemistry and Molecular Biology, Inc.

This article is available online at <https://www.jlr.org>

Abbreviations: AUC, area under the curve; CM, chylomicron; CM^{IA}, chylomicron purified from triglyceride-rich lipoprotein by immunoaffinity; CM^U, chylomicron fraction isolated by ultracentrifugation; CM^{U+IA}, chylomicron purified from CM^U by immunoaffinity; DNL, de novo lipogenesis; FT, flow-through; MIDA, mass isotopomer distribution analysis; NFDM, nonfat dried milk; TAG, triacylglycerol; TRL, triglyceride-rich lipoprotein; VLDL^U, VLDL isolated by ultracentrifugation.

¹A. Gugliucci and J.-M. Schwarz contributed equally as senior authors.

²To whom correspondence should be addressed.

e-mail: jean-marc.schwarz@tu.edu or Jean-Marc.Schwarz@ucsf.edu (J.-M.S.); alejandro.gugliucci@tu.edu (A.G.)

fat [de novo lipogenesis (DNL)] could also be an important contributor to postprandial VLDL levels (6, 7). Additionally, DNL and other metabolic markers, such as LDL-cholesterol and TAG, were significantly reduced in children with metabolic syndrome that underwent a 9 day fructose restriction diet (8, 9).

Postprandial plasma TAGs are derived from two sources. First, dietary TAGs are hydrolyzed into monoacylglycerols and fatty acids are absorbed by the intestine, where they are re-esterified into TAGs, packaged into CMs, and secreted into the lymph before reaching the general circulation (10). Second, hepatic TAGs are synthesized from either free fatty acids that are released by the adipose tissue or synthesized de novo or derived from dietary CM remnants taken up by the liver. These hepatic TAGs are repackaged into VLDL and secreted into the bloodstream (11).

Research into the relative roles and abundances of CM and VLDL particles in the postprandial state has been hindered because of limitations in laboratory methods used to separate these particles. Ultracentrifugation can achieve separation of triglyceride-rich lipoproteins (TRLs) and partial separation of CMs from VLDL, but cannot fully separate particles of overlapping densities, such as small CMs or CM remnants from large VLDL particles and VLDL remnants (12). This technical barrier has limited investigations that aim to characterize: 1) the respective contribution of TAG from the intestines and from the liver to postprandial lipid metabolism; 2) the kinetic aspects, namely the respective turnover rates of CMs versus VLDL particles; 3) the differential clearance

rates of TAG; or 4) the impact of dietary factors, such as carbohydrates, sugar, and branched-chain amino acids, among others, on postprandial lipid metabolism and cardiovascular risk.

To overcome the aforementioned limitations of ultracentrifugation separation, we developed an immunoaffinity method to separate CMs from VLDL (Fig. 1). While alternative immunoaffinity methods exist (13, 14), we needed to obtain and document purer CMs as well as a robust method that would allow for the majority of intact CM particles to be recovered, as they are quite labile. Intact particles contain information regarding the tissue of origin and might allow for the investigation of human intestinal DNL, as has long been predicted in the literature. We generated polyclonal antibodies directed to a C-terminal sequence in ApoB100, which is absent in the ApoB48 sequence. This allowed for the separation of CM and VLDL particles. Antibodies were cross-linked to a protein G resin to create an anti-ApoB100 resin that allowed the isolation of purified CM particles. In the first part of this study, we applied postprandial TRL (δ 1.0063 g/ml, 17 h spin) and impure CM fractions isolated by ultracentrifugation (CM^U ; δ 1.0063 g/ml, 0.5 h spin) to the ApoB100-specific resin to generate purified CMs. In the second part of this study, we further characterized these purified particles; and to illustrate the application of our method, we measured fractional DNL (15) in the purified CM fractions using GC/MS and mass isotopomer distribution analysis (MIDA) (16–19) from samples collected from human volunteers during an 8 h feeding study.

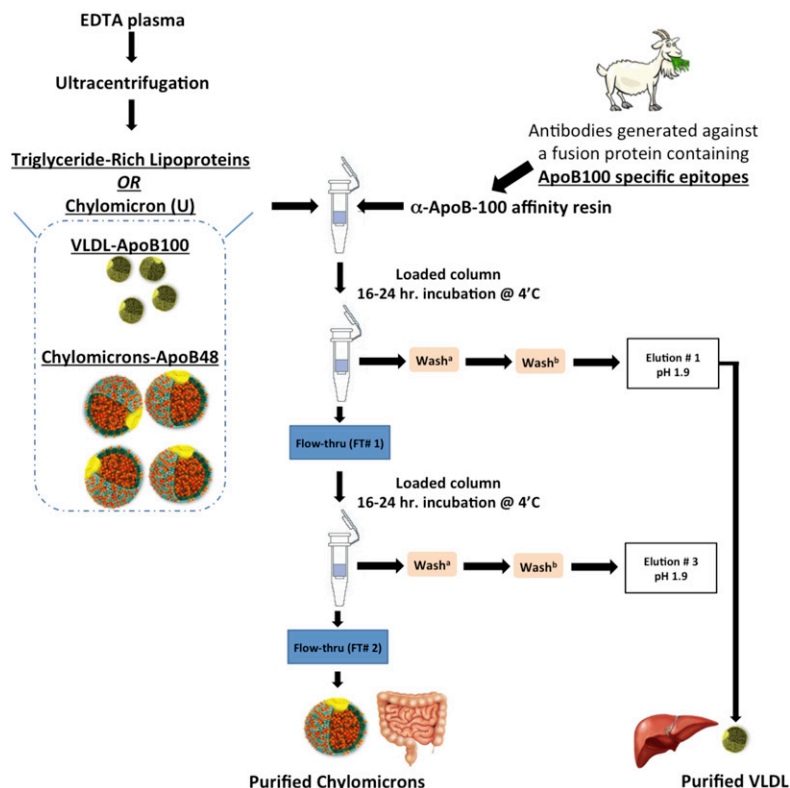


Fig. 1. Schematic of the immunoaffinity protocol for purified postprandial lipoproteins. TRLs or chylomicrons (U)/(CM^U) were isolated from fresh never frozen plasma by ultracentrifugation and applied to the α -ApoB100 immunoaffinity columns as described in the Materials and Methods. Samples were incubated on columns for 16–24 h at 4°C with continuous mixing to collect Elution #1, containing VLDL particles, and Flow-thru #1, containing CMs and some VLDL particles. A second pass of Flow-thru #1 was done to collect purified CMs in Flow-thru #2 and purified VLDL in Elution #3.

Preparation of anti-ApoB100 immunoaffinity resin

We generated ApoB100 immunoaffinity columns to separate CMs from VLDL using a goat antibody raised against ApoB100-specific epitopes purified on an LDL column.

Preparation of the fusion protein and the antiserum

Using the pATH20 vector, we produced a trpE fusion protein, which was used as an antigen for the production of α -ApoB100 antibodies in a goat (20). A 1,862 bp *APOB* fragment was amplified using human genomic DNA (primers: 5'-ctccatattcaaaactagagttagaggg-3' and 5'-attagttctctcccacagtttagc-3'). The product was digested with *Pst*I and *Hind*III. A 784 bp band (*APOB* codons 4,108–4,369) was purified and ligated into pATH20 (21). This was used to transform competent *Escherichia coli* RR1 cells. Cells from positive colonies were grown at 37°C to mid log phase in tryptophan-supplemented medium in 10 ml starter cultures. These were diluted to 500 ml in tryptophan-free medium. After a 2 h incubation, indoleacrylic acid was added to induce expression. After an overnight incubation, the cells were pelleted and protein dissolved in urea/Tris/NaCl buffer. The 66 kDa-fusion protein was purified on preparative 12% SDS-PAGE gels and used to inoculate a goat. A naïve adult goat was given an initial immunization followed by four boosters over a 70 day period. Anti-serum was harvested on day -49, -63, -77, and -84.

Preparation of immunoglobulins

Goat anti-serum was diluted 2-fold and buffered with 100 mM Tris HCl (pH 8.0). Antibodies were precipitated on ice using saturated ammonium sulfate, up to 50%, stirring constantly for 6 h, after which samples were centrifuged at 3,000 g for 30 min at 4°C. The supernatant was removed and the pellet was washed twice and resuspended in PBS. The immunoglobulin solution was then dialyzed in PBS overnight at 4°C.

Preparation of LDL ApoB100 resin

The procedure employed a modified form of the Amino-Link coupling resin protocol (Thermo Fisher Scientific, Waltham, MA). The immobilized protein for the α -ApoB100 affinity column was LDL (ApoB100, δ 1.019–1.063 g/ml) purified from human serum by sequential ultracentrifugation. Four milliliters of LDL (1 mg protein/ml) in 10 mM PBS containing 20% sucrose was diluted 1:2 with 20% sucrose, 100 mM NaHCO₃ (pH 9.0), 500 mM NaCl, and 1 mM EDTA. The final volume of the coupling load was 8 ml. At each step, protein content in the nonbound fractions was analyzed by Coomassie Plus protein assay (Thermo Fisher Scientific) to determine coupling efficiency. Amino Link Plus NaCNBH₃ (sodium cyanoborohydride)-activated resin (Thermo Fisher Scientific) was equilibrated with 10 column volumes of coupling buffer. The coupling load was added to the resin and mixed for 2 h at room temperature, after which the columns were drained and washed with 5 column volumes of coupling buffer, followed by 3 column volumes of 100 mM PBS (pH 7.2). Approximately 50 mM of sodium cyanoborohydride were added to the column and mixed for 2 h at room temperature. The column was drained and washed with 5 column volumes of 1 M Tris-HCl (pH 8.0) to quench the reaction. To reduce the remaining amino groups, 1 M Tris-HCl (pH 8.0) and 50 mM NaCNBH₃ were added to the column and mixed for 2 h at room temperature, then drained. The column was washed with 5 column volumes of 1 M NaCl, drained, then washed with 250 ml 1× PBS (pH 7.6), 1 mM EDTA, and 0.01% sodium azide and stored at 4°C. Three 5 ml columns were made and pooled. The binding efficiencies were consistently >90% and the columns bound approximately 0.56 mg/ml LDL.

Purification of the ApoB100 antibody

The LDL ApoB100 resin prepared as described above (15 ml) was equilibrated with PBS and 1 mM EDTA and added to the immunoglobulin solution and mixed for 48 h at 4°C. Eighty percent of the supernatant was decanted through a 20 ml low pressure column; the other 20% was mixed with the resin and pipetted onto the column and allowed to drain. The column was washed with PBS, 1 M NaCl, and 1 mM EDTA (5 vol) and then with 10 vol of PBS and 1 mM EDTA. Ten milliliters of 100 mM glycine (pH 2.5) were added to the column and incubated for 15 min to elute the antibody. The eluate was collected and the column neutralized with 1 M Tris-Base. The column was then stripped with elution buffer [0.1 M glycine (pH 1.9)] and neutralized with 5 column volumes of 0.1 M phosphate buffer (pH 8.0) and washed with 250 ml of PBS with 1 mM EDTA. The collected eluate was analyzed by Coomassie Plus protein assay to determine purification efficiency and antibody concentration. The flow-through (FT) fraction was reapplied and the procedure above followed; an equal amount of antibody was recovered. The antibody fraction from both preparations was pooled and concentrated for binding to Protein G UltraLink (Thermo Fisher Scientific) using Ultracel 10 kDa MWCO centrifugal filters (Amicon, EMD Millipore, Millipore-Sigma, Billerica, MA). Coomassie Plus protein assay was used to analyze the retentate and filtrate. The combined eluate was 28 ml at a concentration of 0.189 mg/ml or 5.3 mg; the filtrate was 0.00 mg/ml; the retentate was 2 ml at a concentration of 2.83 mg/ml or 5.6 mg, and recovery was ~100%.

Preparation of protein G- α -ApoB100 resin

The coupling and cross-linking of the purified α -ApoB100 antibody to Protein G Ultra Link resin (Thermo Fisher Scientific) were done according to the protocols provided by Thermo Fisher Scientific. The resin was prepared in a 4 ml Bio-Rad Econo column (Bio-Rad, Hercules, CA); samples of each step were taken and checked by the Coomassie Plus protein assay to determine coupling efficiency. Briefly, the protein G resin was equilibrated with 10 column volumes of PBS (pH 7.6). The α -ApoB100 antibody, purified as previously described, was added to the resin (4.5 mg in 2 ml of resin) and mixed overnight at 4°C. A solution of 25 mM disuccinimidyl suberate as a cross-linker was prepared in dimethylformamide and added to the column, which was allowed to come up to room temperature for 30 min. The column was drained and quenched with 2 column volumes of 40 mM Tris (pH 7.4) and then washed with 5 column volumes of each of the following buffers: PBS; 1 M NaCl (pH 7.6); 0.1 M glycine (pH 1.9); PBS and 0.001% NaN₃ (pH 7.6). The coupling efficiency was determined to be 100% and there was no loss of antibody from the cross-linking reaction.

Validation of the immunoaffinity separation method

To determine whether our immunoaffinity method ($n = 4$) was superior to traditional ultracentrifugation separation ($n = 8$), we used fasting and postprandial blood samples collected throughout a 1-¹³C acetate stable-isotope tracer study. From collected samples, we compared fractionated lipoproteins by using Western blots to observe apolipoproteins and by measuring fractional DNL.

Purification of ApoB48-containing lipoprotein from ultracentrifuged plasma samples by α -ApoB100 column

Fresh never-frozen TRL ($\delta < 1.0063$ g/ml, >17 h spin at 40,000 rpm) or CM^U ($\delta < 1.0063$ g/ml, 0.5 h spin at 33,000 rpm) fractions were applied to the protein G- α -ApoB100 affinity resin and incubated overnight (16–24 h) at 4°C with continuous mixing for two consecutive passes (Fig. 1). Freezing samples leads to the degradation of CM particles. The volumes used were in a 1:2 ratio, 200 μ l of equilibrated resin to 400 μ l of sample in a spin column

(Thermo Fisher Scientific). The FT fractions (containing ApoB48 particles) were removed by centrifugation and stored on ice to be reapplied to the same resin after it had been washed, eluted, and re-equilibrated. The resin from pass #1 was washed with 12 column volumes of PBS [1 mM EDTA, 0.5 M NaCl (pH 7.5)] and 12 column volumes of PBS [1 mM EDTA (pH 7.5)]. The resin was eluted with 0.1 M glycine (pH 1.9); VLDLs were eluted twice from columns after a 20 min incubation at room temperature. After the elution, the column was neutralized with 5 column volumes of 0.1 M phosphate buffer (pH 8.0), washed with 10 column volumes of PBS (pH 7.5), and equilibrated with 0.9% NaCl. After equilibration, the FT fraction was reapplied for pass #2. The FT fraction and the elution fractions ("E"; containing ApoB100 particles) were taken at each step for evaluation by Western blot. After the second pass and final elution, the protein G- α -ApoB100 resin was equilibrated with 10 column volumes of 0.9% NaCl and stored at 4°C. We found that two passes were needed for optimal results. Purified CMs obtained from TRLs will be referred to as CM^F and purified CMs obtained from CM^U will be referred to as CM^{U+IA}.

Study participants

Eight healthy volunteers (Table 1) with no history of chronic disease and currently taking no medications were recruited to take part in this study. The study was approved by the Institutional Review Board of Touro University California, Vallejo, CA, which adhered to the World Medical Association Declaration of Helsinki principles. Informed written consent was obtained from all participants before the start of the study.

Feeding study using 1-¹³C sodium acetate stable-isotope tracer

After a 10–12 h fast, participants underwent an 8 h feeding study to achieve a postprandial state, during which 67% of their estimated daily energy requirement was consumed (containing 15% of calories as protein, 35% as fat, and 50% as carbohydrate). For each participant, 1 liter of regular Coca-Cola was mixed with 3.5 g of 1-¹³C sodium acetate (Cambridge Isotopes, Tewksbury, MA) and evenly divided into 17 drinks. In addition, an 18 inch long commercially prepared tuna sandwich was divided into 9. This allowed for the constant oral administration of stable-isotope tracer in this study. After an initial double-sized meal, one meal (one sandwich portion) was consumed every hour for 7 h (Fig. 2). After an initial double-sized drink, one drink was consumed every 30 min. Blood was drawn at baseline and every hour for 7 h after the initial test meal. Specimens were collected in K₂EDTA tubes with added preservatives (gentamicin sulfate, chloramphenicol sodium succinate, aprotinin, sodium azide, trolox, and benzamidine) and kept on ice until they were centrifuged within 30 min of collection (500 g for 10 min at 4°C) to separate plasma, which was stored at 4°C

until the end of the study day (Fig. 2). Processing of samples, which were at no time frozen, began at the end of the study day. To minimize proteolysis of ApoB, samples were kept at a temperature of between 4°C and 12°C with chelating (EDTA) and protease (aprotinin and benzamidine) inhibitors present throughout the procedures.

Isolation of TRLs from plasma

Plasma was collected as described above (n = 8). Four milliliters of plasma were overlaid with a δ 1.0063 g/ml saline solution and centrifuged (Beckman L8-80) at 134,934 g in a Tff45.6 rotor for \geq 17 h at 12°C. The top layer of this fraction, \sim 1.8 ml, was removed by tube slicing for further analysis and will be referred to as TRL.

Isolation of CMs and VLDL using the traditional ultracentrifugation method

A second 4 ml aliquot of plasma was overlaid with a δ 1.0063 saline solution, placed in a Tff45.6 rotor, and centrifuged (Beckman L8-80) at 91,839 g for 30 min at 12°C (n = 8). Approximately 1.5 ml of the sample were removed by tube slicing and referred to as CM^U (CM from ultracentrifugation). The remaining volume was transferred to a fresh tube, overlaid with a δ 1.0063 saline solution, placed in a Tff45.6 rotor, and centrifuged (Beckman L8-80) at 134,934 g for \geq 17 h at 12°C. Tube slicing isolated the top 1.8 ml, the VLDL fraction.

Immunoblotting

SDS-PAGE gels were transferred to PVDF Immobilon-P transfer membrane using the Transblot SD Semidry transfer cell (Bio-Rad) at 25 volts for 20 min per gel. Membranes were blocked using 5% nonfat dried milk (NFDM) in TTBS (0.5% Tween 20 in TBS), pH 7.5, and incubated overnight at 4°C. ApoB100 and ApoB48 (differentiated by their molecular weights) were detected by the anti-ApoB antibody-HRP (ab27622; Abcam, Cambridge, MA) (22) at 1:18,000 in 5% NFDM in TTBS for 2 h at room temperature. ApoB100 was detected by the goat polyclonal antibody generated for this study at 1:2,000 or 0.23 μ g/ml in 5% NFDM in TTBS overnight at 4°C. ApoB100 and ApoB48 were quantified using National Institutes of Health Image J software, and the recovery and purity of each fraction were calculated relative to TRL or CM^U.

Determination of fractional DNL via GC/MS and MIDA

Fractional DNL was determined by measuring biosynthetic rates of palmitate, isolated from fractionated plasma, using stable-isotope tracer methodology via GC/MS and MIDA (17–19). In these experiments, palmitate from TAG was analyzed as a methyl-palmitate derivative (*m/z* 270, 271, and 272). Briefly, chloroform and methanolic-HCl were added to the TAG samples isolated by thin-layer chromatography and incubated at 37°C overnight. Next,

TABLE 1. Anthropometric data

Subject	Sex	BMI	TAG	Chol	HDL-C	Calc. LDL-C
		kg/m ²	mg/dl	mg/dl	mg/dl	mg/dl
1	M	29.5	90	155	33	104
2	M	24	97	209	35	155
3	F	34.0	31	111	37	68
4	M	30.0	89	184	41	125
5	M	24.4	80	157	55	87
6	F	21.0	65	133	50	70
7	F	27.4	170	178	40	105
8	F	27.0	199	182	31	111

TAG, plasma triacylglycerol; Chol, plasma total cholesterol; Calc. LDL-C, calculated plasma LDL-C. LDL-C was calculated using the Friedwald formula, [(Chol – HDL-C) – (TAGs/5)], units are milligrams per deciliter. Cohort #1, subjects 1–4 and cohort #2, subjects 5–8. Samples from cohort #1 underwent ultracentrifugation separation only, whereas samples from cohort #2 underwent separation by both ultracentrifugation and immunoaffinity.

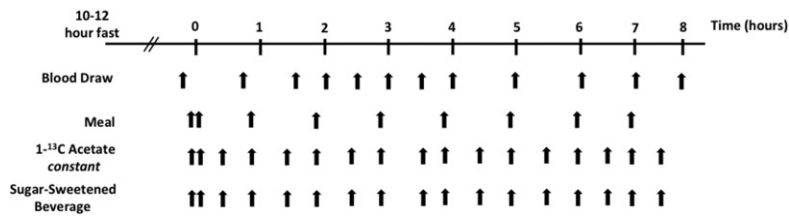


Fig. 2. Stable-isotope study design. Recruited subjects arrived at the Metabolic Research Center after a 10–12 h fast. An intravenous line was placed and a baseline blood draw was taken. Subsequently, subjects were given meals, a sugar-sweetened beverage, and the oral stable-isotope $1\text{-}^{13}\text{C}$ acetate, and blood was drawn as outlined above. We used oral isotopes in a previous study and found that this type of administration was very effective (8).

hexane and 5% NaCl were added to the samples to extract fatty acid methyl esters. The resulting samples were then transferred to autosampler vials for GC/MS analysis. Methyl-palmitate isotopomers were analyzed by an electron ionization GC/MS instrument, Agilent-5973 (Agilent, Santa Clara, CA), operated in positive-ion mode of detection and equipped with a RESTEK Rxi-5ms capillary column (RESTEK, Bellefonte, PA).

Statistical analysis

Data were analyzed using JMP software (SAS, Cary, NC). Differences in mean fractional DNL area under the curve (AUC) were analyzed using two-tailed *t*-test, and differences with $P < 0.05$ were considered statistically significant.

RESULTS

Purification of CMs with traditional ultracentrifugation versus α -ApoB100 immunoaffinity method

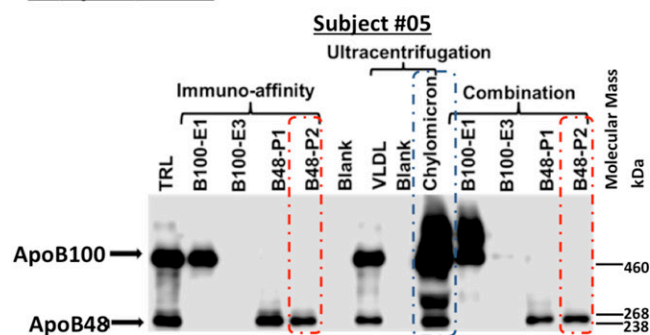
TRL and CM^{U} samples were applied to the α -ApoB100 columns and purified CMs collected (Fig. 1). Western blots were

used to determine the ability of the traditional ultracentrifugation and immunoaffinity methods to purify CMs (Fig. 3). The CM lane demonstrates that the traditional ultracentrifugation method does not separate ApoB48- and ApoB100-containing particles (Fig. 3, blue boxes). Figure 3, red boxes, shows the absence of ApoB100 in CM fractions purified from either TRL or CM^{U} using the immunoaffinity method, CM^{IA} , and $\text{CM}^{\text{U+IA}}$, respectively. Using this technique, we recovered 80–88% of VLDL and 57–90% of CMs, purity was 100% for VLDL and between 90% and 94% for CMs.

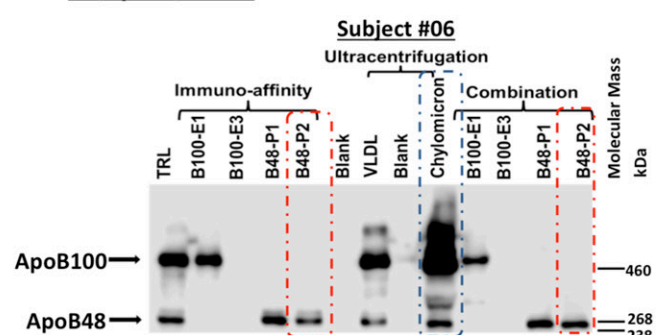
Fractional DNL in TRL, CM^{U} , and VLDL $^{\text{U}}$

To assess previously reported intestinal DNL in CM^{U} and to understand the contribution of contamination by VLDL, we measured and compared fractional DNL in the CM^{U} , TRL, and VLDL obtained by ultracentrifugation (VLDL $^{\text{U}}$) fractions, which demonstrates the inability of ultracentrifugation to purify CMs from VLDL and supports the use our immunoaffinity method to possibly quantify enteral DNL.

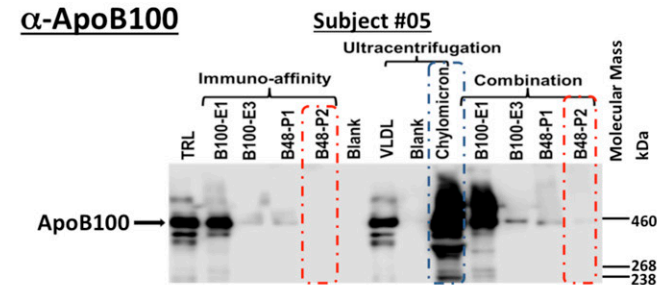
A α -ApoB Total



C α -ApoB Total



B α -ApoB100



D α -ApoB100

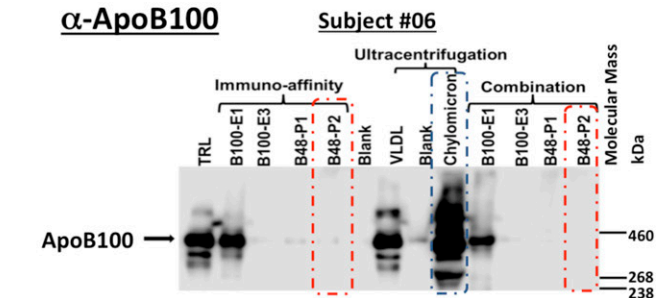


Fig. 3. Western blot analyses of TRL and CM^{U} after application of immunoaffinity columns. A, C: Representative Western blots of TRL, CM^{U} , VLDL $^{\text{U}}$, and purified CM fractions collected at study hour 6, using an ApoB-total antibody to detect both ApoB100 and ApoB48; apolipoproteins found in VLDL and CM particles, respectively. B, D: Representative Western blots of TRL, CM^{U} , VLDL $^{\text{U}}$, and purified CM fractions collected at hour 6 using an ApoB100-specific antibody to detect ApoB100-containing lipoproteins (VLDL). Red boxes outline Flow-thru #2 from the final pass of sample over the immunoaffinity columns. Blue boxes outline the CM^{U} fraction purified by ultracentrifugation. E1, Elution #1; E3, Elution #3; P1, Pass #1; P2, Pass #2.

MIDA allows for the calculation of fractional DNL by measuring the relative distribution of isotopomers of palmitate (M+0, M+1, and M+2; incorporation of 0, 1, or 2 $1\text{-}^{13}\text{C}$ acetyl-CoA, respectively) (23), where acetyl-CoA is the monomer and palmitate is the polymer. We found that the average DNL during the feeding study rose up to $\sim 11\%$ in TRL, up to $\sim 9\%$ in CM^{U} , and up to $\sim 16\%$ in VLDL^{U} (Fig. 4). The mean VLDL^{U} -DNL AUC over 5 h (study time 3–8 h) was greater than the mean TRL-DNL AUC ($73.2 \pm 11.5 \times 5$ h versus $53.9 \pm 6.8 \times 5$ h, $P = 0.012$), while there was a smaller yet significant difference between the mean TRL-DNL AUC versus the CM^{U} -DNL AUC ($53.9 \pm 6.8 \times 5$ h versus $46.6 \pm 6.6 \times 5$ h, $P = 0.0009$). While statistical analyses show that there is a significant difference between the DNL AUC of fractionated samples and TRL, the Western blot analysis (Fig. 3, blue boxes) demonstrated that the traditional ultracentrifugation method resulted in CMs that were heavily contaminated by VLDL, consistent with the CM^{U} fractional DNL measurements.

Fractional DNL in immunoaffinity-purified CM fractions

TAG from the purified CM fractions, CM^{IA} (7 samples per subject, totaling 28 samples), and $\text{CM}^{\text{U+IA}}$ (7 samples per subject, totaling 28 samples), were isolated, from four of the eight subjects, and fractional DNL measured in a subset of subjects whose samples underwent the immunoaffinity separation method. CM^{U} -DNL AUC averaged 40.8 ± 8.2 versus 19.3 ± 8.0 in the purified CM^{IA} fraction, $P = 0.06$. This trend may suggest that the TRL samples applied to the α -ApoB100 columns yielded purer CM particles compared with those obtained by the traditional ultracentrifugation method (Fig. 5). Similarly, fractional DNL results with the CM^{U} fraction subjected to the α -ApoB100 columns indicated purer CM particles ($\text{CM}^{\text{U+IA}}$). The average fractional DNL AUC in these samples was 14.6 ± 4.1 ($n = 4$) (Fig. 5, diamonds). Compared with the averaged CM^{U} -DNL AUC, the $\text{CM}^{\text{U+IA}}$ -

DNL AUC was significantly less (40.8 ± 8.2 versus 14.6 ± 4.12 , $P = 0.015$). Additionally, when average fractional CM^{U} -DNL AUC is compared with the average fractional DNL AUC measured in CMs purified from either TRL (CM^{IA}) or CM^{U} ($\text{CM}^{\text{U+IA}}$) fractional DNL was reduced by $55.7\% \pm 14.6\%$, $P = 0.06$ or $64.7\% \pm 5\%$, $P = 0.015$, respectively.

DISCUSSION

This report describes an immunoaffinity method to effectively purify CMs from VLDL in postprandial human plasma samples. This method now makes the evaluation of the relative contribution of the small intestine versus the liver to postprandial lipid fluxes possible and, in doing so, allows us to address important questions, such as the dietary influences of postprandial lipids on cardiovascular risk. Also, by applying this method to samples from a tracer feeding study, we generated preliminary evidence suggesting that enteral conversion of dietary sugar to fat via DNL can be tested using this methodology.

Two other publications have described the separation of CM and VLDL particles in postprandial samples, each using a set of monoclonal antibodies. These options have their limitations. Heath et al. (13) utilized cyanogen bromide (CNBr)-activated Sepharose conjugated to one of three monoclonal antibodies in the solid phase. This technique lends itself to the possibility of contamination of the CM fraction by VLDL because CNBr-activated Sepharose interacts with amino groups present on lipoprotein particles (14). Moreover, CNBr is quite toxic and volatile, even in small amounts. Sun et al. (14) developed an immunoaffinity protocol that calls for sequential exposure of a sample to three monoclonal antibodies. While it appears that ApoB48 and ApoB100 particles are separated, this method requires a lot of time and sample manipulation, which might lead to sample contamination, degradation, and the misinterpretation of data. We developed an alternative approach employing polyclonal antibodies and immunoaffinity chromatography to successfully purify CMs from VLDL in postprandial plasma samples.

To apply and illustrate a possible application of our immunoaffinity method, we conducted a continuous feeding protocol using test meals containing $1\text{-}^{13}\text{C}$ sodium acetate isotopic tracer. This approach in a larger cohort can be used to test the existence of enteral DNL and its potential contribution to the postprandial lipid profile and associated risk for cardiovascular disease. In each of the studied subjects, we observed increases in fractional DNL during the feeding period in the TRL, VLDL^{U} , and CM^{U} fractions. We reasoned that, in a purer CM sample, DNL would be less than TRL-DNL, VLDL^{U} -DNL, and CM^{U} -DNL, as VLDL would minimally influence CM measurements. The experimental data support this hypothesis: VLDL^{U} -DNL AUC $>$ TRL-DNL AUC $>$ CM^{U} -DNL AUC $>$ CM^{IA} -DNL AUC $>$ $\text{CM}^{\text{U+IA}}$ -DNL AUC ($58.2 > 46.9 > 40.8 > 19.3 > 14.6$, $\times 5$ h, $n = 4$). Furthermore, TRL-DNL served as a reference point because it is a

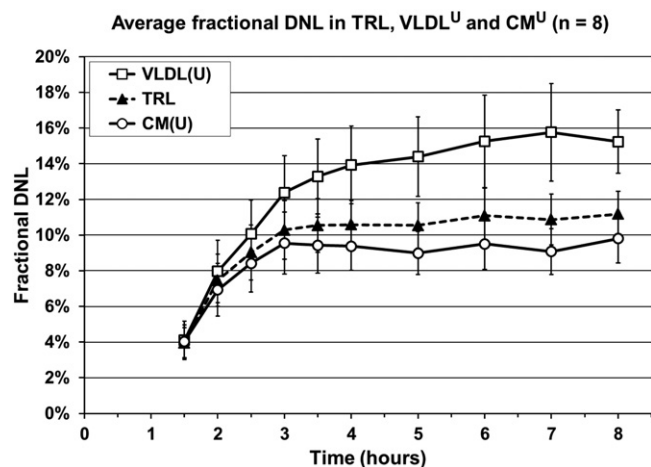


Fig. 4. Average fractional DNL in TRL, VLDL^{U} , and CM^{U} . Average fractional DNL measured in eight healthy adults over an 8 h stable-isotope tracer study. Average DNL AUC $\times 5$ h (study time 3–8 h): TRL, 53.9 ± 6.8 ; VLDL^{U} , 73.2 ± 11.5 ; CM^{U} , 46.6 ± 6.6 (average \pm SEM). DNL AUC p-value, $n = 8$: TRL versus VLDL^{U} , $P = 0.0120$; TRL versus CM^{U} , $P = 0.0009$; VLDL^{U} versus CM^{U} , $P = 0.0051$. VLDL^{U} / $\text{VLDL}(\text{U})$, VLDL obtained by ultracentrifugation; CM^{U} or $\text{CM}(\text{U})$, CMs obtained by ultracentrifugation.

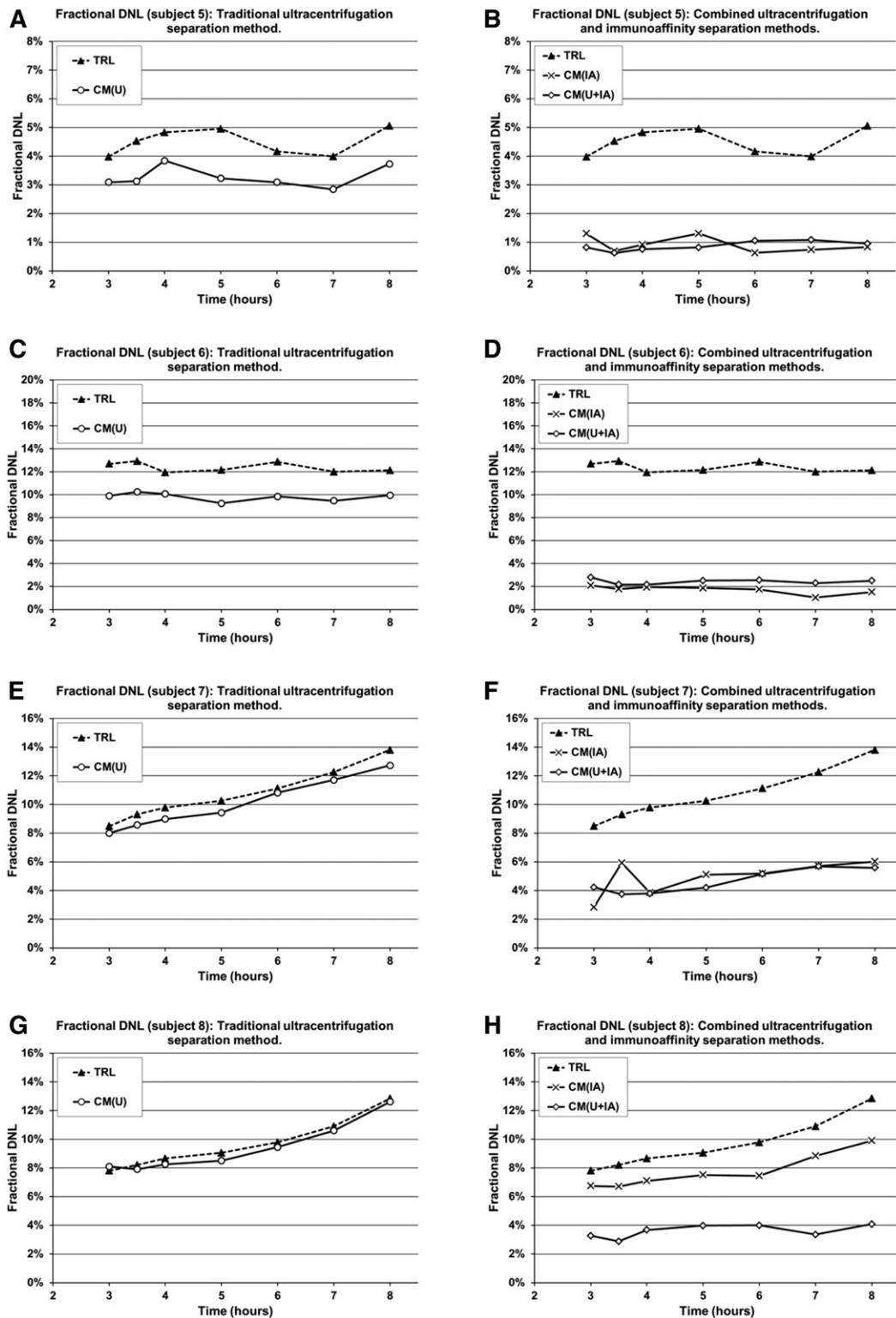



Fig. 5. Individual fractional DNL in traditional ultracentrifugation versus immunoaffinity fractions. Fractional DNL measured in 4 healthy adults (subjects 5–8) over 5 h of stable-isotope tracer study. Mean DNL AUC \times 5 h (study time 3–8 h) \pm standard error of the mean, $n = 4$: TRL, 46.9 ± 8.5 ; CM^{IA} , 19.3 ± 8 ; CM^U , 40.8 ± 8.2 ; CM^{U+IA} , 14.6 ± 4.1 . DNL AUC P -value, $n = 4$: CM^U versus CM^{IA} , $P = 0.0621$; CM^U versus CM^{U+IA} , $P = 0.0153$; CM^{IA} versus CM^{U+IA} , $P = 0.4511$.

composite of VLDL and CM particles. Notably, the MIDA approach based on GC/MS measurements detected fractional DNL in the immunoaffinity-purified CM fractions, CM^{IA} and CM^{U+IA} (Fig. 5). Together these data

demonstrate that the immunoaffinity method more effectively separated CM particles from both TRL and CM^U samples. Additionally, fractional DNL measured in purified VLDL particles isolated by this method was

similar to DNL in particles isolated by the traditional ultracentrifugation method (data not shown). Thus the immunoaffinity protocol not only allows for the purification of CMs but is also an alternate to the traditional VLDL sequential ultracentrifugation purification technique.

While DNL was thought to occur predominately in the liver, some studies have reported intestinal DNL in hamsters (24) and in humans using the ultracentrifugation separation method (25, 26). The data reported here agree, in principle, with those findings. However, our immunoaffinity technique eliminates the potential confounding effect of contamination of intestinal DNL measurements by label from hepatic-derived TAGs, as observed. Hence, our immunoaffinity method combined with MIDA will provide an opportunity to study the relative importance of enteral and hepatic DNL. This method and preliminary observations raise a series of interesting questions: Does diet modulate enteral DNL differently than hepatic DNL? Is the intestinal microbiota a factor in enteral DNL? Does intestinal DNL have a role in metabolic regulation? What is the relative significance of intestinal DNL versus hepatic DNL? Recently, Jang et al. (27) demonstrated murine intestinal conversion of fructose to glucose as a means of mitigating hepatic fructose toxicity, a mechanism that can become overwhelmed by excess fructose consumption, especially in the absence of other foods. Perhaps there is an analogous adaptation in humans. Similarly, as intestinal DNL is evident in hamsters (24), humans might have also adapted the ability to funnel carbons from sugar to fat via DNL, shielding the liver and body from fructose toxicity. While these and many other questions are raised from the data presented here, it is clear that additional research is needed using a larger cohort to address these questions, specifically, mechanistically and physiologically targeted research.

In conclusion, we have shown that CMs (ApoB48 particles) can be purified from VLDL (ApoB100 particles) using an α -ApoB100 immunoaffinity technique that achieves purity (90–94% pure) not possible with the widely employed ultracentrifugation protocol (10% pure). Our method will allow for confident exploration of CM metabolism, devoid of confounding by VLDL contamination interference. It will allow a better understanding of the role of postprandial lipids and explore Zilversmit's (4) postulation that CMs and CM remnants may have a role in atherosclerosis. 

REFERENCES

- Grundy, S. M. 1998. Hypertriglyceridemia, atherogenic dyslipidemia, and the metabolic syndrome. *Am. J. Cardiol.* **81**: 18B–25B.
- Austin, M. A. 1999. Epidemiology of hypertriglyceridemia and cardiovascular disease. *Am. J. Cardiol.* **83**: 13F–16F.
- Austin, M. A. 1989. Plasma triglyceride as a risk factor for coronary heart disease. The epidemiologic evidence and beyond. *Am. J. Epidemiol.* **129**: 249–259.
- Zilversmit, D. B. 1979. Atherogenesis: a postprandial phenomenon. *Circulation.* **60**: 473–485.
- Parks, E. J., R. M. Krauss, M. P. Christiansen, R. A. Neese, and M. K. Hellerstein. 1999. Effects of a low-fat, high-carbohydrate diet on VLDL-triglyceride assembly, production, and clearance. *J. Clin. Invest.* **104**: 1087–1096.
- Schwarz, J. M., S. M. Noworolski, M. J. Wen, A. Dyachenko, J. L. Prior, M. E. Weinberg, L. A. Herraiz, V. W. Tai, N. Bergeron, T. P. Bersot, et al. 2015. Effect of a high-fructose weight-maintaining diet on lipogenesis and liver fat. *J. Clin. Endocrinol. Metab.* **100**: 2434–2442.
- Stanhope, K. L., J. M. Schwarz, N. L. Keim, S. C. Griffen, A. A. Bremer, J. L. Graham, B. Hatcher, C. L. Cox, A. Dyachenko, W. Zhang, et al. 2009. Consuming fructose-sweetened, not glucose-sweetened, beverages increases visceral adiposity and lipids and decreases insulin sensitivity in overweight/obese humans. *J. Clin. Invest.* **119**: 1322–1334.
- Schwarz, J. M., S. M. Noworolski, A. Erkin-Cakmak, N. J. Korn, M. J. Wen, V. W. Tai, G. M. Jones, S. P. Pali, M. Velasco-Alin, K. Pan, et al. 2017. Effects of dietary fructose restriction on liver fat, de novo lipogenesis, and insulin kinetics in children with obesity. *Gastroenterology.* **153**: 743–752.
- Lustig, R. H., K. Mulligan, S. M. Noworolski, V. W. Tai, M. J. Wen, A. Erkin-Cakmak, A. Gugliucci, and J. M. Schwarz. 2016. Isocaloric fructose restriction and metabolic improvement in children with obesity and metabolic syndrome. *Obesity (Silver Spring).* **24**: 453–460.
- Harvey, R. A., and D. R. Ferrier. 2011. Lippincott's Illustrated Reviews: Biochemistry. 5th edition. Wolters Kluwer Health, Philadelphia.
- Taskinen, M. R., and J. Boren. 2015. New insights into the pathophysiology of dyslipidemia in type 2 diabetes. *Atherosclerosis.* **239**: 483–495.
- Lieberman, M., A. D. Marks, and A. Peet. 2013. Marks' Basic Medical Biochemistry: A Clinical Approach. 4th edition. Wolters Kluwer Health/Lippincott Williams & Wilkins, Philadelphia.
- Heath, R. B., F. Karpe, R. W. Milne, G. C. Burdge, S. A. Wootton, and K. N. Frayn. 2003. Selective partitioning of dietary fatty acids into the VLDL TG pool in the early postprandial period. *J. Lipid Res.* **44**: 2065–2072.
- Sun, F., M. Stolinski, F. Shojaae-Moradie, S. Lou, Y. Ma, R. Hovorka, and A. M. Umpleby. 2013. A novel method for measuring intestinal and hepatic triacylglycerol kinetics. *Am. J. Physiol. Endocrinol. Metab.* **305**: E1041–E1047.
- Hellerstein, M. K., R. A. Neese, and J. M. Schwarz. 1993. Model for measuring absolute rates of hepatic de novo lipogenesis and reesterification of free fatty acids. *Am. J. Physiol.* **265**: E814–E820.
- Hellerstein, M. K., J. M. Schwarz, and R. A. Neese. 1996. Regulation of hepatic de novo lipogenesis in humans. *Annu. Rev. Nutr.* **16**: 523–557.
- Hellerstein, M. K., and R. A. Neese. 1999. Mass isotopomer distribution analysis at eight years: theoretical, analytic, and experimental considerations. *Am. J. Physiol.* **276**: E1146–E1170.
- Hellerstein, M. K., M. Christiansen, S. Kaempfer, C. Kletke, K. Wu, J. S. Reid, K. Mulligan, N. S. Hellerstein, and C. H. Shackleton. 1991. Measurement of de novo hepatic lipogenesis in humans using stable isotopes. *J. Clin. Invest.* **87**: 1841–1852.
- Hellerstein, M. K., C. Kletke, S. Kaempfer, K. Wu, and C. H. Shackleton. 1991. Use of mass isotopomer distributions in secreted lipids to sample lipogenic acetyl-CoA pool in vivo in humans. *Am. J. Physiol.* **261**: E479–E486.
- Pullinger, C. R., B. R. Zysow, L. K. Hennessy, P. H. Frost, M. J. Malloy, and J. P. Kane. 1993. Molecular cloning and characteristics of a new apolipoprotein C-II mutant identified in three unrelated individuals with hypercholesterolemia and hypertriglyceridemia. *Hum. Mol. Genet.* **2**: 69–74.
- Mercy, M. R., J. C. Troncoso, and M. J. Monteiro. 1992. A new series of trpE vectors that enable high expression of nonfusion proteins in bacteria. *Protein Expr. Purif.* **3**: 57–64.
- Gugliucci, A., M. Numaguchi, R. Caccavello, and S. Kimura. 2014. Small-dense low-density lipoproteins are the predominant apoB-100-containing lipoproteins in cord blood. *Clin. Biochem.* **47**: 475–477.
- Hellerstein, M. K., and R. A. Neese. 1992. Mass isotopomer distribution analysis: a technique for measuring biosynthesis and turnover of polymers. *Am. J. Physiol.* **263**: E988–E1001.
- Haidari, M., N. Leung, F. Mahbub, K. D. Uffelman, R. Kohen-Avramoglu, G. F. Lewis, and K. Adeli. 2002. Fasting and postprandial overproduction of intestinally derived lipoproteins in an animal

- model of insulin resistance. Evidence that chronic fructose feeding in the hamster is accompanied by enhanced intestinal de novo lipogenesis and ApoB48-containing lipoprotein overproduction. *J. Biol. Chem.* **277**: 31646–31655.
25. Theytaz, F., S. de Giorgi, L. Hodson, N. Stefanoni, V. Rey, P. Schneiter, V. Giusti, and L. Tappy. 2014. Metabolic fate of fructose ingested with and without glucose in a mixed meal. *Nutrients.* **6**: 2632–2649.
26. Surowska, A., S. De Giorgi, F. Theytaz, V. Campos, L. Hodson, N. Stefanoni, V. Rey, P. Schneiter, M. Laville, V. Giusti, et al. 2016. Effects of roux-en-Y gastric bypass surgery on postprandial fructose metabolism. *Obesity (Silver Spring).* **24**: 589–596.
27. Jang, C., S. Hui, W. Lu, A. J. Cowan, R. J. Morscher, G. Lee, W. Liu, G. J. Tesz, M. J. Birnbaum, and J. D. Rabinowitz. 2018. The small intestine converts dietary fructose into glucose and organic acids. *Cell Metab.* **27**: 351–361.e3.